Glycobiology vol. 12 no. 5 pp. 1–13, 2002

Studies on the metal binding sites in the catalytic domain of β1,4-galactosyltransferase

Elizabeth Boeggeman[2,3] and Pradman K. Qasba[1,2]

[2]Structural Glycobiology Section and [3]Intramural Research Support Program-SAIC, Laboratory of Experimental and Computational Biology, NCI-CCR, Building 469, Room 221, Frederick, MD, 21702-1201, USA

Received on December 6, 2001; revised on February 6, 2002; accepted on February 24, 2002

The catalytic domain of bovine β1,4-galactosyltransferase (β4Gal-T1) has been shown to have two metal binding sites, each with a distinct binding affinity. Site I binds Mn^{2+} with high affinity and does not bind Ca^{2+}, whereas site II binds a variety of metal ions, including Ca^{2+}. The catalytic region of β4Gal-T1 has DXD motifs, associated with metal binding in glycosyltransferases, in two separate sequences: D^{242}YDYNCFVFS<u>DVD</u>^{254} (region I) and W^{312}GWGG<u>EDDD</u>^{320} (region II). Recently, the crystal structure of β4Gal-T1 bound with UDP, Mn^{2+}, and α-lactalbumin was determined in our laboratory. It shows that in the primary metal binding site of β4Gal-T1, the Mn^{2+} ion, is coordinated to five ligands, two supplied by the phosphates of the sugar nucleotide and the other three by Asp254, His347, and Met344. The residue Asp254 in the $D^{252}VD^{254}$ sequence in region I is the only residue that is coordinated to the Mn^{2+} ion. Region II forms a loop structure and contains the $E^{317}DDD^{320}$ sequence in which residues Asp318 and Asp319 are directly involved in GlcNAc binding. This study, using site-directed mutagenesis, kinetic, and binding affinity analysis, shows that Asp254 and His347 are strong metal ligands, whereas Met344, which coordinates less strongly, can be substituted by alanine or glutamine. Specifically, substitution of Met344 to Gln has a less severe effect on the catalysis driven by Co^{2+}. Glu317 and Asp320 mutants, when partially activated by Mn^{2+} binding to the primary site, can be further activated by Co^{2+} or inhibited by Ca^{2+}, an effect that is the opposite of what is observed with the wild-type enzyme.

Key words: aspartate motifs/bovine β4Gal-T1/catalytic domain/metal-binding sites/substrate binding

Introduction

Members of the Golgi-resident glycosyltransferase family of enzymes transfer the sugar residue from a sugar-nucleotide donor to the oligosaccharide moiety of glycoproteins and glycolipids. These Golgi enzymes are membrane-bound and have a type II membrane protein topology consisting of a cytoplasmic tail, a hydrophobic transmembrane domain, a stem region, and a globular catalytic domain that faces the Golgi lumen (Paulson and Colley, 1989). β1,4-Galactosyltransferase (β4Gal-T1) from milk catalyzes the transfer of galactose from UDP-α-D-galactose (UDP-Gal) to either free- or glycan-bound *N*-acetylglucosamine (GlcNAc), producing either free- or oligosaccharide-bound GlcNAc (Galβ1-4GlcNAc) (Hill, 1979). With α-lactalbumin (LA), a mammary gland–specific protein, it forms the lactose synthase complex that transfers galactose from UDP-Gal to free glucose to produce lactose (Galβ1-4Glc) (Morrison and Ebner, 1971a).

Although the bovine β4Gal-T1 was the first glycosyltransferase to be isolated and cloned (Narimatsu *et al.*, 1986; D'Agostaro *et al.*, 1989; Shaper *et al.*, 1986; Masibay and Qasba, 1989; Russo *et al.*, 1990), it was not until recently that a family (β4Gal-T2 to β4Gal-T7) of related human and mouse β4Gal-Ts was identified (Lo *et al.*, 1998; Amado *et al.*, 1999). These glycosyltransferases differ in the oligosaccharide acceptor specificities. Only β4Gal-T1 and β4Gal-T2 have lactose synthase activity in the presence of LA (Almeida *et al.*, 1997). β4Gal-T4 has a weak interaction with LA and is involved in the synthesis of glycosphingolipids (Schwientek *et al.*, 1998). β4Gal-T5 has 37% sequence identity to human β4Gal-T1 but has no lactose synthase activity in the presence of LA (Sato *et al.*, 1998a,b). β4Gal-T6, which has a 94% sequence identity with the rat lactosylceramide synthase and transfers galactose from UDP-Gal to glucosylceramide, shows 39% sequence identity to the catalytic domain of the mouse β4Gal-T1 (Nomura *et al.*, 1998). The newly discovered β4Gal-T7 shows 38% sequence identity to the *Caenorhabditis elegans sqv-3* gene (Okajima *et al.*, 1999) and is reported to be involved in the synthesis of proteoglycans (Okajima *et al.*, 1999; Almeida *et al.*, 1999).

The specificities of glycosyltransferases are determined not only with respect to donor and acceptor substrates but also with regard to the nature of the glycosidic linkage (α or β) that they form. The β4Gal-T family members are classified as "inverting" enzymes because they transfer galactose from UDP-α-D-galactose to GlcNAc with an "inversion" of the configuration at the anomeric carbon atom of galactose, generating a β1-4-linked product (Sinnott, 1990). Bovine milk β4Gal-T1 requires Mn^{2+} for the enzymatic reaction (Morrison and Ebner, 1971b; Khatra *et al.*, 1974; Powell and Brew, 1974; Bell *et al.*, 1976). Kinetic studies showed that the enzyme has two metal binding sites and that the occupation of both sites is required for maximum activation (Powell and Brew, 1976). One of the sites binds Mn^{2+} with high affinity but does not bind Ca^{2+}. The other is a low-affinity site that can also bind Ca^{2+} (Powell and Brew, 1976; O'Keeffe *et al.*, 1980). Investigations of the metal ion requirements of the enzyme have shown that Zn^{2+}, Cd^{2+}, Fe^{2+}, and Co^{2+} can also induce activation with lower activities at saturation than that of Mn^{2+}. The DXD motifs, conserved in the family members of the

[1]To whom correspondence should be addressed

glycosyltransferases (Breton *et al.*, 1998; Yuan *et al.*, 1997; Boeggeman and Qasba, 1998; Wiggins and Munro, 1998; Busch *et al.*, 1998; Shibayama *et al.*, 1998, 1999; Zhang *et al.*, 1999; Hodson *et al.*, 2000; Unligil *et al.*, 2000), have been shown to participate in metal binding and catalysis (Boeggeman and Qasba, 1998; Wiggins and Munro, 1998; Busch *et al.*, 1998; Shibayama *et al.*, 1999; Zhang *et al.*, 1999; Hodson *et al.*, 2000; Unligil *et al.*, 2000).

In the catalytic domain of the β4Gal-T family members, two sequence regions, D^{242}YDYNCFVFS<u>DVD</u>^{254} (region I) and W^{312}GWGG<u>EDDD</u>^{320}(region II), contain the DXD motifs. The $D^{242}YD^{244}$ in region I is not a conserved DXD motif in all the β4Gal-T family members; on the other hand, $D^{252}VD^{254}$ and $E^{317}DDD^{320}$ are highly conserved motifs. The kinetic mechanism of β4Gal-T1 has been suggested to be an equilibrium-ordered mechanism, where UDP-Gal and Mn^{2+} form a complex with the enzyme prior to the binding of the sugar acceptor (Khatra *et al.*, 1974; Powell and Brew, 1974). It has also been suggested that the binding of the substrates to the enzyme–Mn^{2+} complex occurs via a random equilibrium mechanism (Bell *et al.*, 1976). The interaction of the enzyme–Mn^{2+} complex with UDP-Gal has been studied by circular dichroism, and the data indicate that a conformational change occurs on the binding of UDP-Gal to the enzyme-Mn^{2+} complex (Geren *et al.*, 1975) protecting one Trp residue from UV light–induced destruction (Clymer *et al.*, 1976).

Although the crystal structure of the catalytic domain of bovine β4Gal-T1, with and without UDP, has been determined at a 2.4 Δ resolution (Gastinel *et al.*, 1999), it did not provide the exact location of the sugar acceptor or that of Mn^{2+}. In our laboratory, we have determined the crystal structure of the complexes of bovine β4Gal-T1 and mouse α-LA in the presence of Mn^{2+} with various acceptor substrates, at 2 Δ resolution (Ramakrishnan and Qasba, 2001). These show that the Mn^{2+} ion is coordinated with five atoms; two of these are the pyrophosphate ionic oxygen atoms of the sugar nucleotide, and the remaining three atoms are the Cδ of Asp254, the Nε2 atom of His347, and the Sδ atom of Met344 of β4Gal-T1. The structures reveal a conformational change to have occurred within the region comprising residues 345–365 of β4Gal-T1 from the structure obtained by Gastinel *et al.* (1999) (conformation I) to the structure (conformation II) we found (Ramakrishnan and Qasba, 2001). This change positions His347 of the region in such a way that it can bind the Mn^{2+} ion, which subsequently can bind to the phosphates of the UDP-Gal. The second metal binding site was never identified in the LS, UDP-Gal and Mn^{2+} complex even though 17 mM $MnCl_2$ was used during crystallization. The sequence region II, W^{312}GWGG<u>EDDD</u>^{320}, has a loop structure that is similar in conformations, I and II, with subtle differences. In conformation II, the side chain orientation of Trp314 allows it to interact with GlcNAc. Asp318 and Asp319 of the $E^{317}DDD^{320}$ sequence motif, localized in the loop structure, are also involved in GlcNAc binding. Asp320 does not appear to directly bind GlcNAc (Ramakrishnan and Qasba, 2001).

In the present study, using site-directed mutagenesis we investigated the involvement of residues Asp242, Asp244, Asp252, Asp254, His347, and Met344 in metal-ion binding and catalysis**.** Mutation of any of these residues, except Asp242 and Asp244, affect the activity of the enzyme. The kinetic properties of the wild-type and mutated β4Gal-T1 show that among the residues Asp254, His347, and Met344, which coordinate Mn^{2+} (Ramakrishnan and Qasba, 2001), only Asp254 and His347 are important for metal binding. Met344 can be replaced with alanine or glutamine with only a partial loss of enzyme activity. In addition, Glu317 and Asp320 mutants show an effect on their activities that is opposite to the wild-type enzyme when partially activated by Mn^{2+} and subsequently treated with Ca^{2+} or Co^{2+} ions.

Results

Expression and site-directed mutagenesis of β4Gal-T1

The catalytic domain of the *N*-terminal deleted bovine β4Gal-T1, residues 130–402 (recombinant β4Gal-T1), and its mutants were expressed in *Escherichia coli* as nonfusion proteins with an 11 amino acid *N*-terminal extension using standard procedures (Ausubel *et al.*, 1987) as previously described (Boeggeman *et al.*, 1993, 1995). The final yield of the purified folded mutant proteins was comparable to the yield of recombinant β4Gal-T1. Sodium dodecyl sulfate–polyacrylamide gel electrophoresis (SDS–PAGE) analysis of the purified and refolded mutant proteins showed a single protein band corresponding to a molecular weight of 33 kDa of β4Gal-T1. Secondary structure analysis by Fourier-transformed infrared spectroscopy (Keiderling *et al.*, 1999) showed that the mutants and the wild-type β4Gal-T1 have the same secondary structure (data not shown).

Involvement of residues Asp254, Met344 and His347 in metal binding

In the absence of metal ions, β4Gal-T1 does not catalyze the transfer of galactose from UDP-Gal to GlcNAc. The structure of β4Gal-T1·UDP·LA·Mn^{2+} (Ramakrishnan and Qasba, 2001) showed that of the two Asp residues of the $D^{252}VD^{254}$ motif, only the carboxylate oxygen of Asp254 coordinates with Mn^{2+}. On the other hand, Asp252 binds only to the galactose moiety of UDP-Gal in the donor substrate binding pocket of β4Gal-T1 (Ramakrishnan *et al.*, 2002). Also, in the β4Gal-T1·UDP-Glc·LA·Mn^{2+} complex, Asp252 binds to the glucose moiety of UDP-Glc (Ramakrishnan *et al.*, 2001). Although the mutation of Asp252 completely abolishes the catalytic activity of the enzyme, the mutant D252N binds to an UDP-agarose column like the enzymatically active wild type. Also, the mutants of Asp254, D254E and D254N barely retain 0.01% of the catalytic activity of β4Gal-T1 (Table I). Due to the low levels of activity, the kinetic parameters for these mutants could not be obtained with confidence. The results are consistent with the finding that these residues, Asp252 and Asp254, are highly conserved among all the members of the β4Gal-T family (Breton *et al.*, 1998).

M344A mutant, in the presence of Mn, retained 54% of the wild-type enzyme activity, whereas the mutant M344Q retained only 15% of the activity (Table I). In the presence of Co^{2+}, however, M344Q was fourfold more active than β4Gal-T1. Comparison of the sequences of the catalytic domain of the family members of β4Gal-T shows that Met344 is only present in Gal-T1, T2, T3, and T4 (Lo *et al.*, 1998), and is substituted by serine in other β4Gal-T family members. The substitution of His347 either by glutamic acid, glutamine, aspartic acid, or asparagine abolishes the activity of the enzyme almost

Table I. Metal ion-dependent activity of the mutants of the primary metal binding site of β4Gal-T1

Protein	Mn^{2+}	Co^{2+}
β4Gal-T1	100*	8.10
D254A	ND	ND
D254E	0.01	ND
D254N	0.01	ND
M344A	54.50	6.15
M344Q	15.37	31.08
H347E	0.105	0.405
H347D	0.02	0.085
H347Q	0.28	1.21
H347N	0.07	0.360

Specific activities of the recombinant β4Gal-T1 and the mutants of the primary metal binding site, in the presence of either Mn^{2+}or Co^{2+} ion. Mutation of aspartic acid residues at positions 242 and 244 gave activities similar to the wild type (not shown). Assay conditions were 0.2 mM UDP-Gal, 25 mM GlcNAc, and either 5 mM Mn^{2+} or 5 mM Co^{2+}. ND, not detectable. Numbers represent % relative to 100*, which is 6.66 μmoles/min/mg of protein of β4Gal-T1.

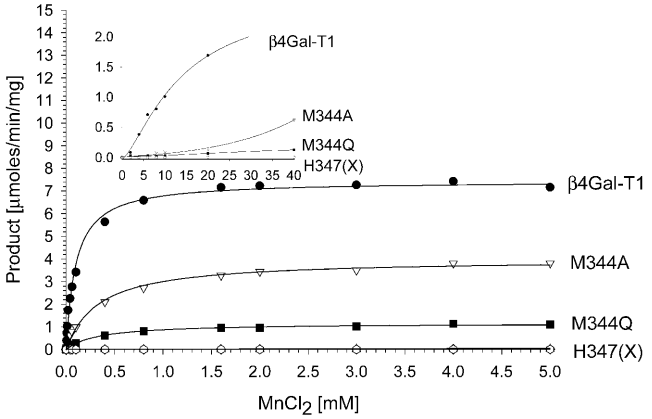

Fig. 1. Mn^{2+}-dependent enzyme activity of the wild-type β4Gal-T1 and mutated proteins. Assays were carried out in duplicates at fixed concentrations of GlcNAc (25 mM) and UDP-Gal (0.2 mM) and at varied concentrations of Mn^{2+}. The insert shows the sigmoidal dependence of enzyme activity at low concentrations of Mn^{2+} (0–40 μM) for β4Gal-T1 and the methionine mutants M344A and M344Q. The enzymatic activity of the histidine (H347X) mutants is very low compared to β4Gal-T1.

completely when Mn was used (Table I). However, Co^{2+} then becomes the preferred metal ion when His347 is substituted either by glutamic acid, glutamine, asparagine or aspartic acid (Table I). Comparison of the sequences of this region among the family members of β4Gal-T shows that His347 is also a highly conserved residue.

Effect of Mn ion on the enzymatic activity of Met344 mutants

Enzyme activities of the wild-type and the Met344 mutants were measured at Mn^{2+} concentrations from 0 to 5 mM and at fixed concentrations of GlcNAc and UDP-Gal. The Mn ion–dependent activation of M344A and M344Q showed a sigmoidal behavior (Figure 1). At least 20 μM Mn^{2+} is required to detect the activation of Met mutants, compared to about 4 μM for the wild-type enzyme. The mutants clearly require a higher Mn concentration for activation than the wild-type protein (Figure 1). The enzymatic activities of β4Gal-T1 and M344A at Mn^{2+} concentrations from 0 to 5 mM fitted well to a rate equation describing two metal binding sites, I (high affinity) and II (low affinity). Mutant M344A, compared to the wild-type, shows a fourfold lower binding affinity for site I and no effect on the affinity for site II (Table II). The data for M344Q did not fit well to Equation 3 (see *Materials and methods*), which describes two metal binding sites. However, the rate equation for a single metal binding site, Equation 4 (see *Materials and methods*), gave a better fit (Table II), showing higher affinity for Mn^{2+} but with a sevenfold reduction in the associated velocity.

Effect of Co on the enzymatic activity of M344 and H347 mutants

We tested Co^{2+}, Zn^{2+}, and Cd^{2+} for the activation of the wild-type and mutant enzymes and found that Co activated the mutants more than the other metal ions. The Met344 and His347 mutants are activated to some extent by Co^{2+} (Table I). In the presence of either Mn^{2+} or Co^{2+}, His347 mutants show drastically reduced enzymatic activity. However, the mutants H347E, H347Q, and H347N show four- to fivefold increased activity in the presence of Co^{2+} as compared to Mn^{2+} (Table I). The M344A mutant is 10% less efficient in the presence of Co^{2+} than in the presence of Mn^{2+} (Table I). Surprisingly, M344Q is twofold more active in the presence of Co^{2+} than in the presence of Mn^{2+} and is fourfold more active than recombinant β4Gal-T1. The enzyme activities of mutants were measured at

Table II. Mn^{2+} or Co^{2+} activation parameters of β4Gal-T1 and mutated proteins

Metal	Parameter	Units	β4Gal-T1	M344A	M344Q*
Mn^{2+}	K_1	μM	26 " 3	112 " 0.1	NF
	K_2	μM	870 " 85	916 " 20	315 " 9.3
	V_1	μmoles/min/mg	3.6 " 0.2	1.8 " 0.3	NF
	V_2	μmoles/min/mg	7.5 " 0.26	4.2 " 0.22	1.0 " 0.02
Co^{2+}	K_d	μM	46.07 " 2	53.36 " 3	1926 " 10
	V	μmoles/min/mg	0.98 " 0.02	0.906 " 0.03	7.02 " 10

Kinetic parameters for $MnCl_2$ (0 to 5 mM) from the fitted curves were obtained by Enzfitter (Biosoft) using Equation 3, describing two metal binding sites (see *Materials and methods*). Mn^{2+} data could not be fitted (NF) to Equation 3 for the mutant M344Q*. The data for M344Q* are fitted to Equation 4, describing metal binding to a single site. The values for the parameters for Co^{2+} were obtained by fitting the data, for the lower activating concentration range (400 μM), to Equation 4. Assays were carried out in duplicates at 0.2 mM UDP-Gal and 25 mM GlcNAc.

Co^{2+} concentrations from 0 to 5 mM, at fixed concentrations of UDP-Gal (0.2 mM) and GlcNAc (25 mM). Under these conditions, Co^{2+} was observed to enhance the activity of β4Gal-T1 and of the mutant, M344A, with increasing concentrations up to 250 µM. Above 0.5 mM, it was inhibitory (Figure 2A). In contrast, the histidine mutants show activation when Co concentrations were between 200 µM and 5 mM (Figure 2B). The mutant M344Q at Co^{2+} concentration of 3 mM attains at least three times more activity than β4Gal-T1 before any inhibition in the enzyme activity is observed (Figure 2A). The inhibition by Co^{2+} at higher concentrations may be the result of its binding to more than one site or a denaturation of the proteins at these concentrations. The activity profile with Co^{2+} between the concentrations of 0–400 µM for β4Gal-T1 and the mutants M344A and M344Q fitted well to a rate equation describing a single metal binding site (Table II). The binding affinity for Co^{2+} (K_d) and the associated velocity (V) were similar for the mutant M344A and the wild-type β4Gal-T1. In contrast, for M344Q the K_d for Co^{2+} was 38-fold higher. Thus, it appears that the substitution of Met344 with Ala neither affects the dissociation constant (K_d) for Co^{2+} nor the associated velocity (V), whereas substituting it with Gln reduces the Co^{2+} affinity by 42-fold but increases the velocity by 7-fold.

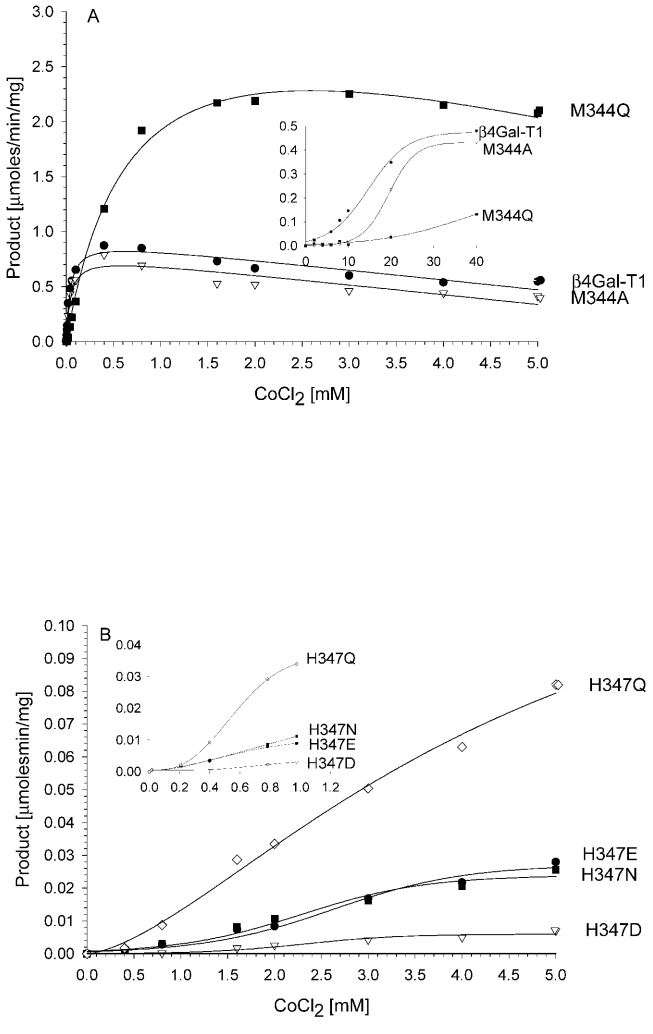

Fig. 2. The effect of increasing concentrations of Co^{2+} on *N*-acetyllactosamine synthesis. (**A**) The methionine mutants; (**B**) the histidine mutants. The insert in **A** shows the activation of methionine mutants and β4Gal-T1 at 0–40 µM Co^{2+}. The insert in **B** shows the activation of the histidine mutants at 0–1 mM Co^{2+}. Enzyme assays were carried out at fixed concentrations of GlcNAc (25 mM) and UDP-Gal (0.2 mM) and varied concentrations of Co^{2+} (0 µM to 5 mM).

Binding of wild-type β4Gal-T1 and mutants to the UDP-agarose column in the presence of different concentrations of Mn^{2+}

To determine the interactions of the residues Met344, Asp254, and His 347 with Mn^{2+} in β4Gal-T1, we tested the Mn^{2+}-dependent binding of the mutants of these residues on UDP-agarose columns and compared the results with that of the enzymatically active protein β4Gal-T1. The mutant proteins, compared to the wild type, required higher concentrations of Mn^{2+} to bind to the UDP-agarose column. In the presence of 25 mM Mn^{2+}, H347D binds to the UDP-column with lesser affinity than the enzymatically active β4Gal-T1 (Figure 3). Moreover, H347D does not bind to the affinity column if the concentration of the metal is reduced in the equilibration buffer to either 5 or 1 mM (Figure 3). In contrast, M344A binds to UDP-agarose as tightly as the wild type only in the presence of 5 and 25 mM Mn^{2+} and not in the presence of 1 mM Mn^{2+} (Figure 3). The mutant D254N does not bind to the UDP-agarose column at any of the Mn^{2+} concentrations tested (Figure 3). On the other hand, the mutant D252N shows Mn^{2+}-dependent binding to the UDP-agarose like the wild type β4Gal-T1 (Figure 3), suggesting that Asp 252 is not involved in Mn^{2+} binding.

UDP-Gal kinetic parameters for β4Gal-T1 and M344A

The bisubstrate reactions can utilize either sequential (ordered or random) or ping-pong (double displacement) mechanisms, which are distinguished by steady-state analyses in which the concentrations of two substrates are independently varied. Because M344Q and His347 mutants showed lower levels of Mn^{2+}-dependent activity and the kinetic parameters could not be determined with confidence, the parameters for only β4Gal-T1 and M344A were obtained (Table III). Galactose transfer to GlcNAc by β4Gal-T1 and M344A was measured at a fixed concentration of GlcNAc (25 mM) and at UDP-Gal concentrations varying from 0.025 mM to 0.2 mM and different fixed concentrations of $MnCl_2$. The double reciprocal plots of velocity versus UDP-Gal at various fixed concentrations of $MnCl_2$ gave a series of intersecting lines as previously observed (Powell and Brew, 1974) (not shown). In each case, the data fitted best to Equation 1 (see *Materials and methods*), indicating a symmetrical sequential or random equilibrium mechanism. Table III shows that mutating Met344 to Ala344 does not significantly change the true K_m value for UDP-Gal, whereas the K_m for Mn^{2+} increases about threefold and the k_{cat} is reduced by a third.

Mutants of $E^{317}DDD^{320}$ sequence that affect β4Gal-T1 enzymatic activity

The $E^{317}DDD^{320}$ motif is a part of the sequence of region II, $W^{312}GWGGEDDD^{320}$, conserved among the β4Gal-T family members. Site-directed mutagenesis of glutamic acid at position 317 and aspartic acid residues at positions 318, 319, and 320 showed that all these residues are important for catalysis (Table IV). Substituting Asp318 or Asp319 with asparagine, alanine, or glutamic acid abolishes the enzymatic activity almost completely (legend to Table IV); the kinetic parameters for these mutants could not be determined.

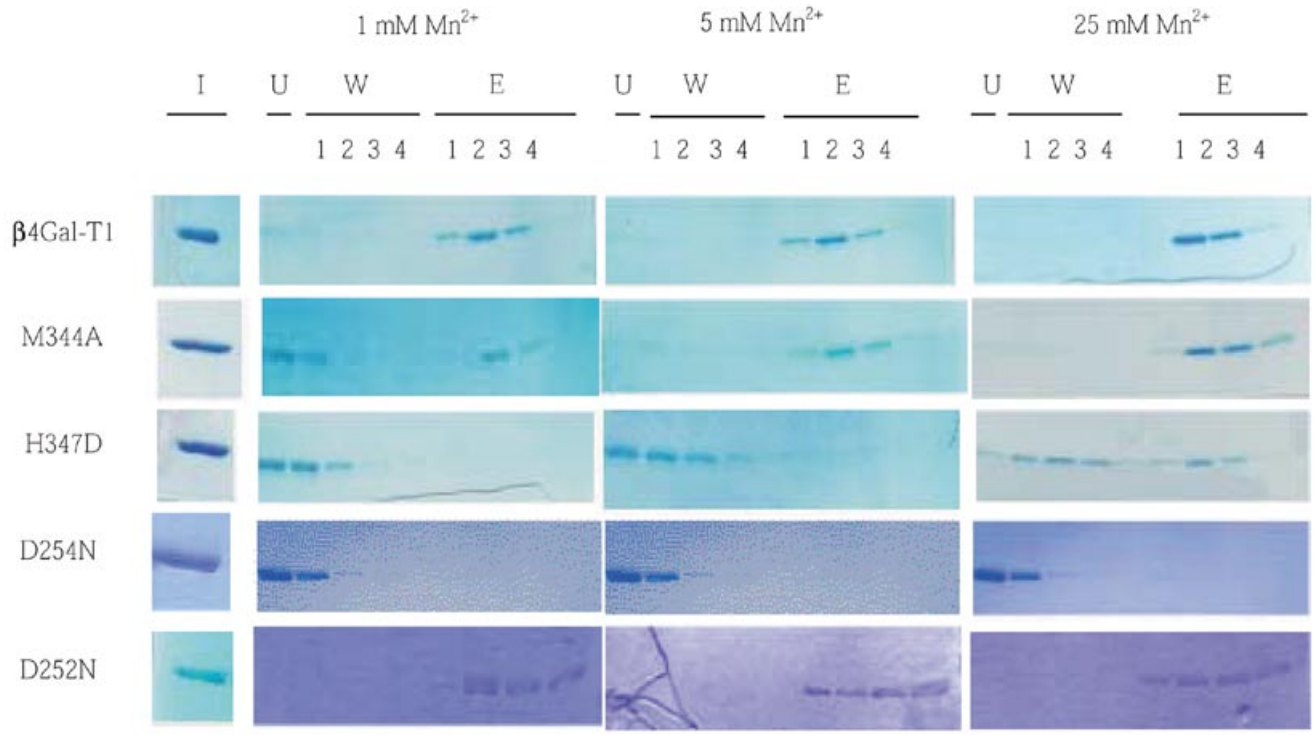

Fig. 3. SDS–PAGE analysis of wild-type β4Gal-T1 and mutated proteins. The renatured proteins of wild-type β4Gal-T1, M344A, H347D, D254N, and D252N were bound to and eluted from UDP-agarose columns as described under *Material and methods*. Aliquots of each fraction were analyzed on gels and proteins visualized by Coomassie blue staining. I is the input sample, U is unbound, W is wash, and E is the eluted sample. The amounts of the input sample (I) loaded on the columns were the same under the three equilibration buffers tested, which contained either 1, 5, or 25 mM $MnCl_2$. The wild type remains bound at all concentrations of Mn^{2+} tested and it is eluted (E) in the presence either of 1, 5 or 25 mM Mn^{2+}. M344A at 1 mM Mn^{2+} binds less efficiently, and a portion of the protein remains in the unbound and the wash fraction (U and W). H347D does not bind to the UDP-agarose column at either 1 or 5 mM Mn^{2+} (U and W) and shows reduced binding at 25 mM Mn^{2+} (U, W, and E). D254N does not bind to the UDP-agarose column (U and W). On the other hand, the mutant D252N binds to the column as the wild type does, and it is eluted (E) in the presence either of 1, 5, or 25 mM Mn^{2+}.

Table III. Kinetic parameters for β4Gal-T1 and M344A

	Parameters	β4Gal-T1	M344A
UDP-Gal	K_{md} (μM)	37 ± 7	26 ± 4
	K_{id} (μM)	26.09 ± 4.5	0.188 ± 0.001
	V_{max} (μmoles/min/mg)	5.91± 0.6	1.82 ± 0.23
	k_{cat} (s^{-1})	3.24	1.00
	$k_{cat}/K_{md} * K_i$ (s^{-1} μM^{-2})	0.095	0.96
$MnCl_2$	K_m (μM)	63.70 ± 0.01	195 ± 1
	K_i (μM)	0.913 ± 0.010	0.040 ± 0.016
	$k_{cat}/K_m * K_{id}$ (s^{-1} μM^{-2})	0.0019	0.0272

Data calculated from the double reciprocal plots for the transfer of galactose to GlcNAc at variable concentrations of UDP-Gal, from 0.025 mM to 0.2 M and $MnCl_2$, from 0.3 mM to 1.6 mM at a fixed concentration of GlcNAc (25 mM) (Figure 3). The data was fitted to Equation 1 using the Enzfitter program from Biosoft.

Table IV. Metal ion–dependent activity of the mutants of the putative secondary metal binding site of β4Gal-T1

Protein	Mn^{2+}	Co^{2+}
β4Gal-T1	100*	8.10
E317A	0.01	ND
E317D	9	2.05
E317Q	0.01	ND
D320A	8	ND
D320E	18	4.83
D320N	1	15.44

Specific activities of the recombinant β4Gal-T1 and the mutants of the putative secondary metal binding site, in the presence of either Mn^{2+} or Co^{2+} ion. Mutation of Asp318 and Asp319 abolished the enzyme activity (not shown). Assay conditions were 0.2 mM UDP-Gal, 25 mM GlcNAc, and either 5 mM Mn^{2+} or 5 mM Co^{2+}. ND, not detectable. The numbers represent % of 100*, which is 6.66 μmoles/min/mg of β4Gal-T1 protein.

Effect of Mn on the enzymatic activity of mutants Glu317 and Asp320

A change of glutamic acid residue at position 317 lowers the activity of β4Gal-T1; specifically, a change to Asp reduces the enzyme activity to 9% compared to β4Gal-T1 (Table IV). Substitution of Glu317 by Ala or Gln abolished the enzymatic activity completely, indicating that both the carboxylate group and the length of the side chain are critical for the activity. A conservative substitution of Asp with Glu at position 320 results in the retention of about 18% of the Mn-dependent enzymatic activity of the β4Gal-T1. Introduction of Ala or Asn at the same position lowered the Mn-dependent enzyme activity by

92% and 99%, respectively. Thus, the correct length of the side chain carrying the carboxylate group at position 320 is also important for activity. The Mn-dependent activity curves of β4Gal-T1 and of the mutants Glu317 and Asp320 are also sigmoidal in behavior (Figure 4A). The mutants, E317D, D320E, and D320N, show reduced response at lower metal ion concentration compared to M344 mutants and require higher Mn^{2+} ion concentration to activate the enzyme compared to the wild type (Figure 4A). The mutants are not activated by 20 µM Mn^{2+}, whereas the activity of the wild type can be measured even at 4 µM Mn^{2+} concentration (Figure 1). The Mn^{2+} concentration-dependent (0–5 mM) activity data of the mutants, at fixed concentrations of UDP-Gal (0.2 mM) and GlcNAc (25 mM), did not fit well into a rate equation describing the two metal binding sites in the case of E317D and D320E mutants (Table V). The D320N mutant, however, showed five- and eightfold increase in the K_1 and K_2 values, respectively, over the values for β4Gal-T1 (data not shown). The equation describing a single binding site for Mn gave a better fit for all the mutants (Table V). Mutants E317D, D320E, and D320N showed a 4- to 17-fold increase in the metal dissociation constant, K_d, compared to the wild type.

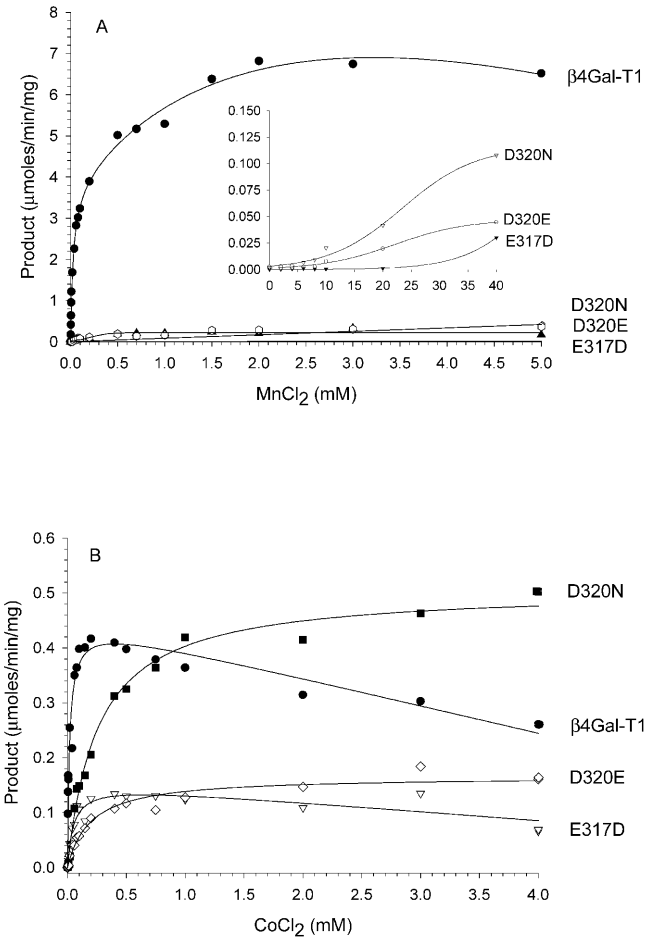

Fig. 4. Mn^{2+}- and Co^{2+}-dependent enzyme activity of β4Gal-T1 and the mutants of the $E^{317}DDD^{320}$ region. Assays were carried out at fixed concentrations of GlcNAc (25 mM) and UDP-Gal (0.2 mM) and at varied concentrations of $MnCl_2$ (0 µM to 5 mM) (**A**) or at varied concentrations of $CoCl_2$ (**B**) (0 µM to 4 mM). The insert in **A** shows the sigmoidal dependence of enzyme activity at low concentrations of Mn^{2+} (0–40 µM) on Glu317 and Asp320 mutants.

Table V. Mn^{2+} or Co^{2+} activation parameters of β4Gal-T1 and mutated proteins of $E^{317}DDD^{320}$ region

	Mn^{2+}		Co^{2+}	
	K_d	V	K_d	V
β4Gal-T1	61.0 " 3	5.8 " 0.15	10.16 " 0.3	0.35 " 0.01
E317D	237.0 " 44	0.25 " 0.002	41.23 " 3.26	0.14 " 0.01
D32ED	1023.0 " 500	0.43 " 0.06	178.0 "1 1	0.16 " 0.003
D320N	233.0 " 95	0.47 " 0.04	295.0 " 25	0.55 "0.05

Kinetic parameters from the fitted curves were obtained by Enzfitter (Biosoft) using Equation 4, describing metal binding to a single site (see *Materials and ethods*). Dissociation constant K_d (µM) and its associated velocity, V (µmoles/min/mg protein) are presented. Assays were carried out in duplicates at 0.2 mM UDP-Gal, 25 mM GlcNAc, and either 0–5 mM $MnCl_2$ or 0–4 mM $CoCl_2$.

Effect of Co^{2+} on Glu317 and Asp320 mutants

A change in the glutamic acid residue at position 317, as mentioned, lowers β4Gal-T1 activity. Mutant E317D retains about 2% of the Mn-dependent activity in the presence of Co^{2+} (Table IV). A conservative substitution of Asp by Glu at position 320 also retains about 5% of the Mn-dependent enzymatic activity of β4Gal-T1. A change to Asn, however, results in a higher enzyme activity in the presence of Co^{2+} than in the presence of Mn^{2+} (Table IV and Figure 4B). The enzyme activities at Co^{2+} concentrations between 0 mM and 4 mM, at fixed concentrations of UDP-Gal (0.2 mM) and GlcNAc (25 mM) did not fit well to the rate equation describing two metal binding sites. The rate equation describing a single metal binding site did fit better to the data (Table V). The K_d values for E317D do not change significantly compared to wild type; however, the metal binding constant, K_d, for D320E and D320N shows an18-fold and 30-fold increase, respectively.

Effect of Co^{2+} and Ca^{2+} at a low Mn^{2+} concentration on the activation of Glu317 and Asp320

It has been shown previously that at low Mn^{2+} ion concentrations, Co^{2+} inhibits the activity of milk β4Gal-T1 (Powell and Brew, 1976). In the presence of a fixed Mn^{2+} concentration (20 µM), the recombinant β4Gal-T1 is inhibited with increasing concentrations of Co^{2+} behaving exactly like milk β4Gal-T1 (Figure 5A). Displacement of Mn^{2+} by Co^{2+} in the wild-type enzyme produces an enzyme–metal complex with lower activity causing enzyme inhibition (Powell and Brew, 1976). With increasing concentrations of Co^{2+}, Mn^{2+} is displaced from the high-affinity binding site, thus inhibiting the enzyme (Figure 5A). In strong contrast, Co^{2+} activates the mutants D320E, D320N, and E317D at 100 µM Mn^{2+} (Figure 5A). These results indicate that Co^{2+} is a more effective cofactor for these mutants compared to wild-type β4Gal-T1.

Ca^{2+} has been shown to bind to the low-affinity metal binding site and not to the high affinity binding site of milk β4Gal-T1 (Powell and Brew, 1976). It cannot by itself stimulate milk β4Gal-T1 (Powell and Brew, 1976). The presence of low concentrations of Mn^{2+} is essential for Ca^{2+} to stimulate

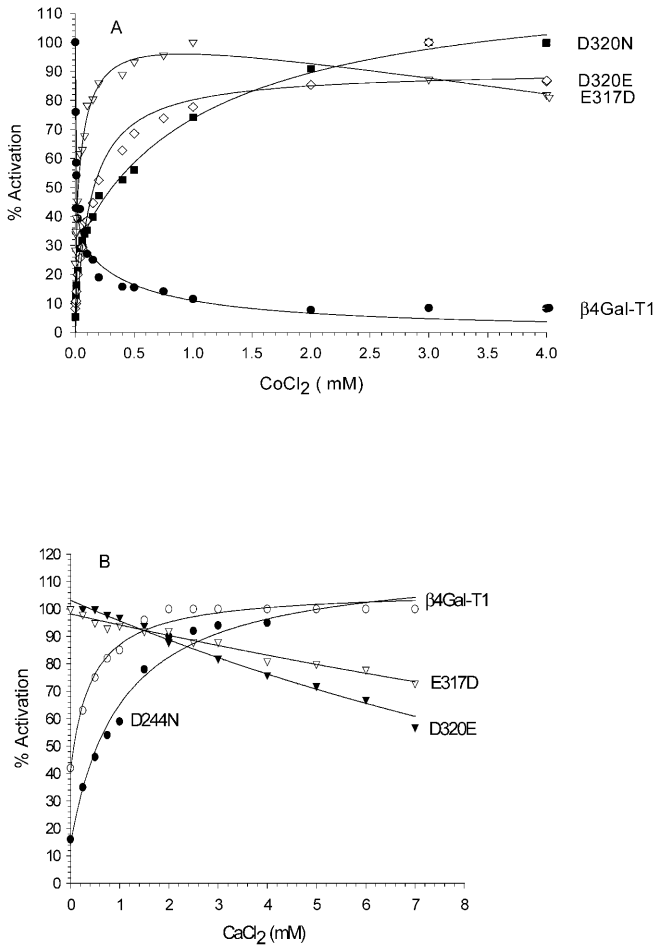

Fig. 5. The effect of Co^{2+} and Ca^{2+} at low concentrations of Mn^{2+} on the activity of β4Gal-T1 and mutants. The assays were carried out at fixed concentrations of GlcNAc (25 mM) and UDP-Gal (0.2 mM) in the presence of low concentrations of Mn^{2+} and at varied concentrations of $CoCl_2$ (**A**) or $CaCl_2$ (**B**). **A** shows inhibition of β4Gal-T1 by Co^{2+} in the presence of 20 μM Mn^{2+} and activation of E317D, D320E, and D320N by Co^{2+} at 100 μM Mn^{2+}. **B** shows the activation of β4Gal-T1 and D244N by Ca^{2+} at 10 μM Mn^{2+}. At higher Mn concentrations (100 μM), Ca^{2+} inhibits the activity of E317D and D320E.

milk β4Gal-T1 (Powell and Brew, 1976) (Figure 5B). The presence of at least two metal binding sites in recombinant β4Gal-T1 is confirmed by the observation that at low Mn^{2+} concentrations (10–20 μM), β4Gal-T1 and the mutant D244N (which behaves like wild type) could be activated by Ca^{2+} (Figure 5B). In contrast, Ca^{2+} did not activate mutants E317D and D320E at low Mn^{2+} concentrations (10–20 μM) (data not shown). In fact, Ca^{2+} had an inhibitory effect on the activity of E317D and D320E at 100 μM Mn^{2+} (Figure 5B). Clearly, in E317D and D320E, the Ca^{2+}-binding site is altered, because the metal ion cannot activate the enzyme even when Mn^{2+} is present at low concentrations.

Kinetic parameters for GlcNAc and UDP-Gal for Glu317 and Asp320 mutants in the presence of Mn^{2+}

The initial velocity data for β4Gal-T1 and for the mutants were obtained at saturating concentrations of Mn^{2+} (10 mM) with varying concentrations of UDP-Gal and a series of fixed concentrations of GlcNAc (Table VI). The data were analyzed using the equations (see *Materials and methods*) that represent the sequential symmetrical initial velocity pattern (Equation 1) or the asymmetric initial velocity pattern (Equation 2). The data for the mutant E317D did not fit well to Equation 1, which is associated with an ordered or random equilibrium mechanism. Equation 2, associated with a ping-pong mechanism, gave a better fit where the value for K_i was zero. The K_m for GlcNAc does not change in the mutant E317D, whereas the K_m for UDP-Gal increases 2-fold compared to β4Gal-T1 (Table VI). Using Eq. 1, the true K_m values for UDP-Gal (K_{md}) and GlcNAc (K_{ma}) were determined for the D320 mutants and compared to the wild type. The K_m for UDP-galactose increased fivefold for D320N, but it decreased to a third in the mutant D320E (Table VI). The equilibrium dissociation constant, K_{id}, for UDP-Gal increased by about 1.5- to 3-fold in these mutants. The K_m for GlcNAc for the mutants D320E and D320N, compared to the wild type, showed values 11- and 151-fold higher, respectively. The turnover number, k_{cat}, however, was reduced, resulting in a 240- to 700-fold decrease in the catalytic efficiency ($k_{cat}/K_{ma} * K_{id}$). k_{cat}, can be influenced by both the rate-limiting acceptor binding and the product release steps; therefore, the specificity constants ($k_{cat}/K_{md} * K_{ia}$ or $k_{cat}/K_{ma} * K_{id}$), which combine rate and binding, are a measure of the stability of the transition state complex. Thus, extending the side chain length of Asp320 indirectly affects the binding of the acceptor and the binding of UDP-Gal to a lesser degree. It also affects the interaction between the enzyme and the substrate in the transition state during the catalytic mechanism.

Table VI. Kinetic parameters for β4Gal-T1 and $E^{317}DDD^{320}$ mutants

Substrates	Parameters	β4Gal-T1	D320E	D320N	E317D*
UDP-Gal (μM)	K_{md}	40.91 ± 5	11.79 ± 0.09	220 ± 23	77.63 ± 3.36
	K_{id}	10.23 ± 1.35	15.35 ± 0.29	33 ± 9	0
GlcNAc (mM)	K_{ma}	2.74 ± 0.85	31.12 ± 0.87	422 ± 15	2.86 ± 0.12
	K_{ia}	0.65	40.51	63.3	0
	V_{max} (μmoles/min/mg)	8.41 ± 1.094	0.47 ± 0.01	3.57 ± 0.11	0.54 ± 0.001
	k_{cat} (s^{-1})	4.62	0.25	1.96	0.29
	$k_{cat}/K_{md} * K_{ia}$ (s^{-1} mM^{-2})	173	0.523	0.140	*

These values were determined at 10 mM Mn^{2+} and varied concentrations of GlcNAc (7.5–50 mM) and UDP-Gal (200–2000 μM). K_{md} and K_{id} are the true K_m and dissociation constant for the donor, respectively. K_{ma} and K_{ia} are the true K_m and dissociation constant for the acceptor. Because $K_{md} * K_{ia} = K_{ma} * K_{id}$, the values for K_{ia} were calculated from the equation $K_{ma} * K_{id} / K_{md}$. *The data for E317D fits to Equation 2, describing a ping-pong mechanism were K_i is zero.

Discussion

Many glycosyltransferases require exogenous divalent cations for their activities and possess specific binding sites for such ions. The DXD motifs in this class of enzymes were suggested to be involved in the metal binding and were also implicated in sugar nucleotide binding (Boeggeman and Qasba, 1998; Busch *et al.*, 1998; Wiggins and Munro, 1998; Unligil *et al.*, 2000). Alignment of the sequences of the catalytic domain of β4Gal-T family members shows that DXD sequence motifs are located within the two sequences, region I, D^{242}YDYNCFVFS<u>DVD</u>^{254}, and region II, W^{312}GWGG<u>EDDD</u>^{320} (Figure 6). Mutagenesis and kinetic analysis of the mutants presented herein showed that Asp242 and Asp244 mutants in region I gave similar activities as the wild-type protein, whereas only the $D^{252}VD^{254}$ motif from region I (Table I) and $E^{317}DDD^{320}$ from the sequence region II (Table IV) are important for β4Gal-T1 activity (Boeggeman and Qasba, 1998;).

This study, using kinetics and binding affinity analysis, shows that of the three protein residues, Asp254, Met344 and His347, that have been identified by X-ray crystallography to coordinate the Mn^{2+} ion (Figure 7) (Ramakrishnan and Qasba, 2001), Met344 coordinates the metal less strongly. This situation is similar to the metal binding site of azurins where Cu^{2+} is coordinated to three strong protein ligands (two histidines and one cysteine) and weakly to a fourth ligand (methionine) (Messerschmidt *et al.*, 1998). Substituting Met344 with alanine or glutamine does not completely abrogate the activity of the protein. It reduces the activity by 45% or 85%, respectively. The mutants M344A and M344Q have about a third to one-fifth affinity for manganese at site I (Table III). Also, the mutant M344A, compared to the wild type, required higher concentrations of Mn^{2+} to bind to the UDP-agarose column (Figure 3), showing it has a weaker affinity for Mn^{2+}. Although M344A has a lower affinity for Mn, the equilibrium dissociation constant for UDP-Gal binding to the enzyme–Mn^{2+} complex, the K_{id}, is decreased and there is a small but significant decrease in the k_{cat} (Table III).

From the metal binding studies on β4Gal-T1, it is apparent that Co^{2+} and Mn^{2+} bind to site I in a similar way, as evidenced by the K_1 values (Table II). Mn^{2+} binding to site II results in activation (Figure 1), whereas Co^{2+} binding results in an inhibition at higher concentrations of the metal ion (Figure 2A). Mutation of Met344 to Gln344 perturbs the properties by decreasing the specific affinity for Co^{2+} while increasing the velocity V_1 about sevenfold (Tables I and II). A change of Met344 to Gln344 restricts the accommodation of the preferred Mn^{2+} ion at the primary metal binding site. However, the mutation may favor local Co^{2+} coordination in a way that stabilizes the transition state complex during catalysis, increasing the velocity of the reaction. The data show that mutating Asp254 and His347 almost completely abolish the enzymatic activity of the protein (Table I), and the mutants D254N and H347D do not bind to the UDP-agarose column in the presence of 1 and 5 mM Mn^{2+} remaining in the unbound fraction (Figure 3). These results show that these residues are strongly coordinating to Mn^{2+}. We crystallized both the mutant proteins, H347E and M344A, in the presence of Co, and their structures are being determined.

The $E^{317}DDD^{320}$ sequence localized in the conserved sequence W^{312}GWGG<u>EDDD</u>^{320} (region II) also contains the DXD motif, which is a potential site for the coordination of divalent cations (Boeggeman and Qasba, 1998). Substituting Asp318 or Asp319 with either asparagine or alanine or glutamic acid almost totally abrogated the activity (Boeggeman and Qasba, 1998) (Table IV), and it was not possible to analyze the kinetic parameters for these mutants. The results presented by Zhang *et al.* (1999) also show that mutating Asp318 with either asparagine or glutamic acid results in 0.1% of the activity of the wild-type protein. This region in the two structures, conformation I and II, also shows differences as evidenced by the side chain orientation of Trp314 (Figures 7A and 7B). In conformation II, the orientation of the side chain of Trp314 is such that it can make hydrophobic interactions with GlcNAc (Figure 7B), as well as with the galactose moiety of UDP-Gal (not shown) and a hydrogen bond with the oxygen atom of the phosphate group of the sugar nucleotide (Ramakrishnan and Qasba, 2001). An earlier study showed that Trp314 is very important for catalysis (Aoki *et al.*, 1990), which is consistent with the structural evidence. The crystal structures of β4Gal-T1and LA in complex with

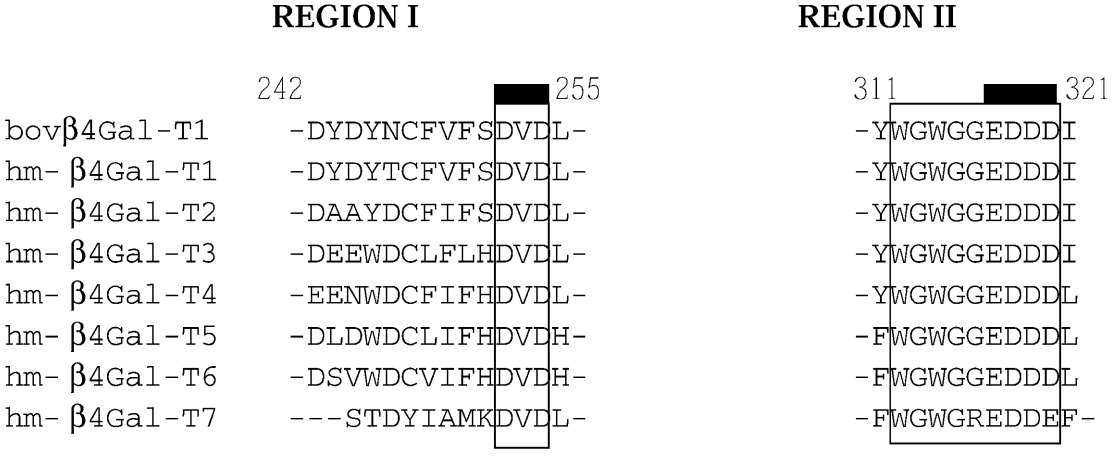

Fig. 6. Sequence comparisons of the two DXD regions in the catalytic domain of β4Gal-T family members. Regions I (residues 242–255) and II (residues 311–321) of bovine β4Gal-T1 and seven human homologs. The conserved residues are boxed and the gaps in the sequence are shown as dashes. The DXD motifs are shown below the black boxes.

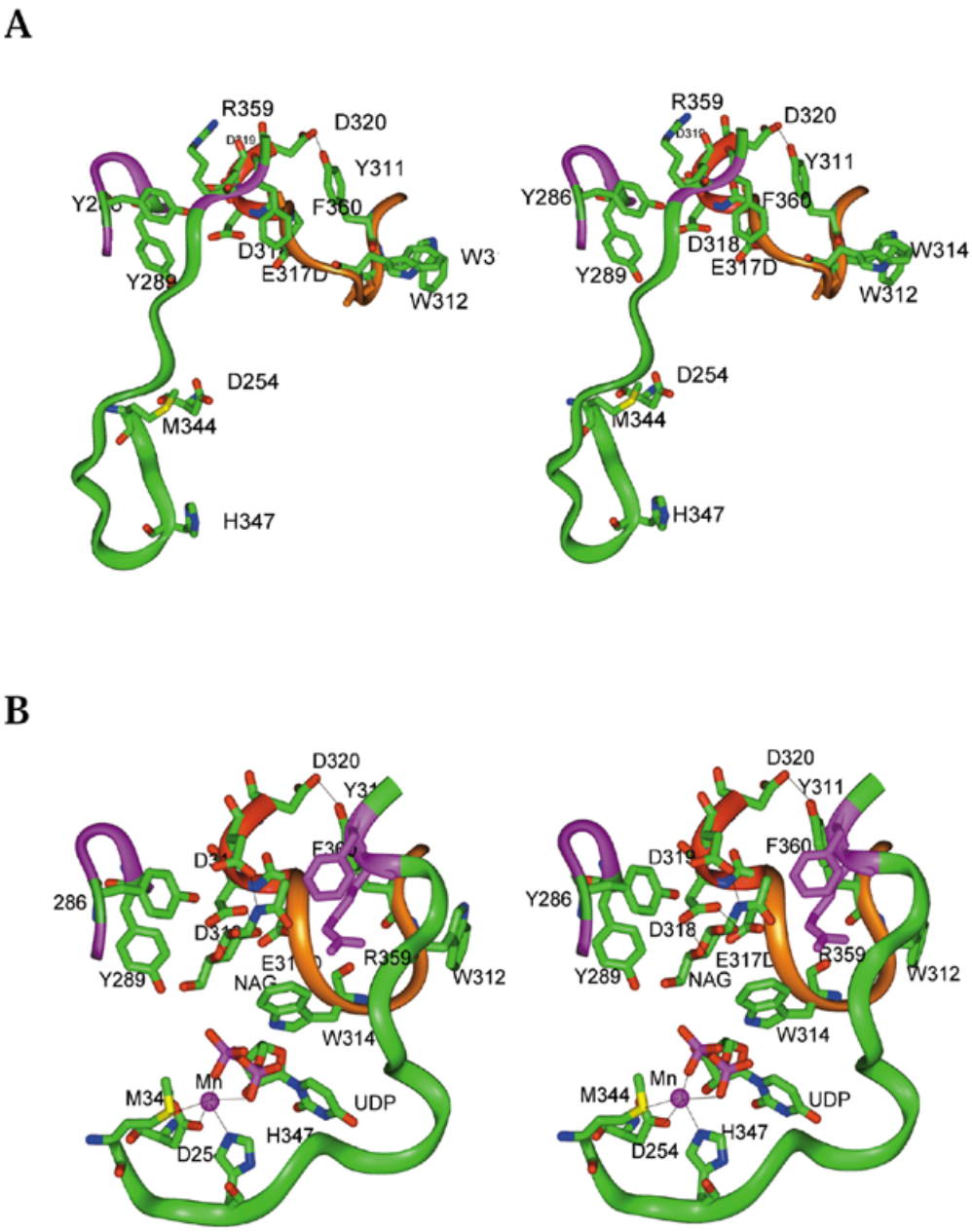

Fig. 7. Stereo diagram of the flexible loop of β4Gal-T1 in conformations I and II. The overall structure of β4Gal-T1 in the two conformations, I and II, is the same and for comparison, the orientation of Tyr 286 and Tyr 289 in the two structures (**A** and **B**) are shown (purple ribbon). However, the structures differ in the flexible loop of β4Gal-T1, residues 345–365 (green ribbon) and the loop region (residues 311–320) (orange ribbon). The $E^{317}DDD^{320}$ sequence region in the loop is shown in red. **A** shows the structures of these regions in conformation I (PDB file; 1FGX). The flexible loop is folded in a way that it covers the sugar binding site and does not show the metal binding pocket in β4Gal-T1. **B** shows the structure of these regions in conformation II (PDB file; 1J8X) (Ramakrishnan and Qasba, 2001). The flexible loop (green ribbon) folds in a way that it creates the UDP-Gal, GlcNAc, and metal binding sites in β4Gal-T1. In this conformation, Mn^{2+} coordinates with UDP through two phosphate ionic oxygen atoms and also coordinates with the side chains of the ligands, D254, H347, and M344. The residues Asp318 and Asp319, localized in the loop region (orange ribbon), bind directly to GlcNAc. In the loop region, Tyr 311 is hydrogen bonded to Asp320 in both conformations, I and II, while the orientation of the side chain of Trp314 is different in the two conformations. A portion of the hydrophobic pocket surrounding the acceptor is shown in purple (residues Arg359 and Phe360).

GlcNAc or Glc show that the carboxylate oxygens of Asp 318 and Asp 319 are hydrogen bonded to the monosaccharide (Ramakrishnan and Qasba, 2001). The carboxylate oxygen of Asp318 forms hydrogen bonds with O3 and O4 of GlcNAc (or Glc) (Figure 7B) (Ramakrishnan and Qasba, 2001). Furthermore, the interactions of *N*-butanoyl-GlcN with the Gal-T1 molecule in the *N*-butanoyl-GlcN-Gal-T1-LA complex are quite similar to the interactions of GlcNAc in the Gal-T1-LA-GlcNac complex (Ramakrishnan *et al.*, 2001).

In recent experiments using photoaffinity-labeled GlcNAc, Asp318 has been identified as the residue that binds the sugar acceptor (Hatanaka *et al.*, 2001). Loss of activity associated

with the substitution of Asp318 or Asp319 with either asparagine or alanine or glutamic acid is also consistent with the structural evidence (Ramakrishnan and Qasba, 2001) and the mutational data of Zhang *et al.* (1999). However, the interpretation of the kinetic data presented by Zhang *et al.* (1999), which states that Asp318 does not directly affect GlcNAc binding, is not consistent with the structural and photoaffinity-labeling data. Mutation of Asp320 also affects the activity; in particular when it is substituted by asparagine. It then prefers Co above Mn as a metal ion. Substitution of Asp320 with glutamic acid, however, results in the retention of about 18% of the Mn^{2+}-dependent activity of the wild type (Table IV). The mutation of Asp320 lowers the affinity for UDP-Gal and more strongly reduces the affinity for GlcNAc. This mutation, however, does not affect the metal binding to the high affinity site (K_1) for Mn. In the crystal structure, Asp320 is not shown to make any contact with GlcNAc (Figure 7B). The carboxylate group of Asp320 is hydrogen-bonded with Tyr311 in both conformations I and II (Figures 7A and 7B). Substituting Tyr311 with glycine results in an increase in K_m for GlcNAc by 1,000-fold and to a lesser extent (35-fold) the K_m for UDP-Gal (Aoki *et al.*, 1990). The hydrogen bond between Asp320 and Tyr311 is likely to help stabilize the loop structure of the sequence region W^{312}GWGG<u>EDDD</u>^{320}, the region that is directly involved in GlcNAc binding and catalysis. Because the D320E mutant retains only 18% of the enzyme activity, the carboxylate group of the glutamic acid may still form a weak hydrogen bond with the hydroxyl group of Tyr311, stabilizing (albeit less efficiently) the loop structure.

Though our data are in agreement with the conclusion that the residues of the E^{317}DDD^{320} motif do not constitute the high-affinity metal binding site (Zhang *et al.*, 1999), they do however show that mutating Glu317 and Asp320 affect the Ca^{2+}- or Co^{2+}-dependent activation. In the absence of Mn^{2+}, Ca^{2+} does not stimulate the enzyme activity of either the wild type or the mutants of Asp242 or Asp244. The wild-type protein and the mutants where the E^{317}DDD^{320} site has not been altered can however be activated by a Ca ion in the presence of low amounts of Mn (Figure 5B). In contrast, Ca^{2+} inhibits the mutants of the E^{317}DDD^{320} region, E317D and D320E at higher Mn^{2+} concentrations (Figure 5B). Because the ionic radius of Ca^{2+} is larger (0.99 Δ) than that of Mn^{2+} (0.80 Δ), Ca^{2+} may not fit in the mutated E^{317}DDD^{320} region. Co^{2+}, on the other hand, may be fitting better in the mutated region because it is seen to activate these mutants when low concentrations of Mn^{2+} are present (Figure 5A). One water molecule has been seen in the center of the loop structure that contains the sequence E^{317}DDD^{320} hydrogen-bonded to Glu317 and the amino nitrogen of Asn356, which could be a potential second metal ion site (Ramakrishnan and Qasba, 2001). Interestingly, there is some sequence identity between the sequence motif of $\underline{W}^{314}\underline{GG}$EDD<u>DI</u>Y^{322} of β4Gal-T and the sequence motif $\underline{W}^{368}\underline{GG}$AGK<u>DI</u>F^{376} of *Serratia* protease. The latter also adopts a loop conformation in the protein, and has been shown to coordinate a Ca^{2+} ion (Figure 8) (Baumann *et al.*, 1995). At present we do not have any structural data for metal binding to the $\underline{W}^{314}\underline{GG}$EDD<u>DI</u>Y^{322} region, but our data show that E317D and D320E or N behave differently toward Ca^{2+} and Co^{2+} activation compared to the wild type. Because the second metal binding site of β4Gal-T1 is a low-affinity binding site, either high concentrations of Mn^{2+} or high concentrations of Ca^{2+} with low concentrations of Mn may be required during crystallization to trap and localize the second metal ion. The mutants described herein are being investigated further for the localization of the second metal binding site of β4Gal-T1.

Materials and methods

Restriction enzymes were from New England Biolabs (Beverly, MA). The Plasmid Mini Preparation Kit was from Qiagen (Santa Clarita, CA). Ampicillin , UDP-Gal, and UDP-agarose

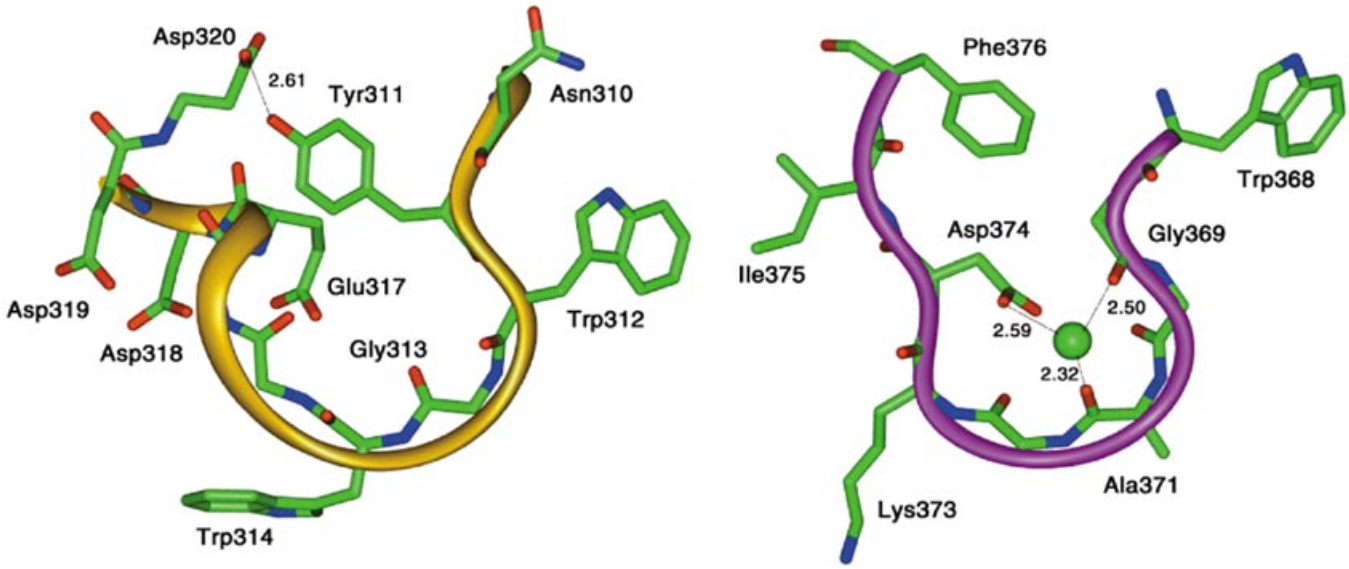

Fig. 8. Structures of the putative second metal binding site in β4Gal-T1 (left) and of the Ca^{2+} binding site in *Serratia* protease (right). The conserved sequence region II of β4Gal-T1, $\underline{W}^{314}\underline{GG}$EDD<u>DI</u>Y^{322}, and the sequence of the Ca^{2+} binding loop of *Serratia* protease, $\underline{W}^{368}\underline{GG}$AGK<u>DI</u>F^{376} (PDB file; 1SRP), show similar residues (underlined) and loop structures.

were from Sigma (St. Louis, MO). pET23a vector and BL21 (DE-3) / pLysS competent cells were from Novagen (Madison, WI). *E. coli* XL2-Blue ultracompetent cells were from Stratagene (La Jolla, CA). AG1-X8 resin, chloride form, 200–400 mesh was from Bio-Rad (Hercules, CA). Taq DNA polymerase and polymerase chain reaction nucleotide mixes were obtained from Boehringer Mannheim.

Bacterial strains and growth conditions

Bacterial growth and transformation and plasmid isolation were carried out by standard procedures (Ausubel *et al.*, 1987). Plasmid pEGT-d129, which encodes the catalytic domain (residues 130–402) of bovine β4Gal-T1, was used as the plasmid template for point mutations. Both wild-type and mutant β4Gal-T1 were expressed in *E. coli* XL2-Blue ultracompetent cells. All the clones were grown in Luria-Bertani medium (LB) containing 50 μg/ml ampicillin at 37°C (Boeggeman *et al.*, 1993, 1995).

Site-directed mutagenesis

The protocol used for site-directed mutagenesis was from Clontech Laboratories (Transformer Site-Directed Mutagenesis Kit). All the mutants were constructed using the plasmid pEGT-d129, containing a *Bam* HI / *Eco* RI fragment of β4Gal-T1, cloned into pET23a (Boeggeman *et al.*, 1993). The transformation process included a selection primer, pNotApa, which was employed to introduce a unique restriction site in pEGT-d129 for further selection. The mutagenic primers were used to introduce the desired mutations. Amplifications of both the parental and mutated strands were accomplished in a repair-deficient *E. coli* strain, BMH71-18 muts. After digesting the parental plasmid with the selection-specific restriction enzyme (*Not I*), the mutant plasmids were amplified and cloned in

E. coli XL2-Blue ultracompetent cells and BL21 (DE3)/pLysS competent cells (Boeggeman *et al.*, 1993, 1995). The mutagenic primers were from Genosys Biotechnologies or Recombinant DNA Laboratory (NCI, Frederick). The nucleotide sequences of the mutagenic primers used for mutagenesis are:

- D242N: 5′ pGAGGCCTTGAAG*AAC*TATGACTACAACTGC-3′
- D242A: 5′ pGAGGCCTTGAAG*GCC*TATGACTACAACTGC-3′
- D242E: 5′ pGAGGCCTTGAAG*GAA*TATGACTACAACTGC-3′
- D244N: 5′ pGAGGCCTTGAAGGACTAT*AAC*TACAACTGC-3′
- D244A: 5′ pGAGGCCTTGAAGGACTAT*GCC*TACAACTGC-3′
- D244E: 5′ pGAGGCCTTGAAGGACTAT*GAA*TACAACTGC-3′
- D252N: 5′ pGCTTTGTGTTTAGC*AAT*GTCGACCTCATCCCA-3′
- D252A: 5′ pGTGTTTAGC*GCT*GTCGACCTCATCCCAATG-3′
- D252E: 5′ pGTGTTTAGC*GAA*GTCGACCTCATCCCAATG-3′
- D254N: 5′ pGTGTTTAGCGATGTG*AAC*CTCATCCCAATGA-3′
- D254A: 5′ pGTGTTTAGCGATGTC*GCC*CTCATCCCAATGA-3′
- D254E: 5′ pGTGTTTAGCGATGTC*GAA*CTCATCCCAATGA-3′
- E317Q: 5′ pGGGGCTGGGGAGGT*CAA*GATGATGACATTTA-TAAC-3′
- E317A: 5′ pGGCTGGGGAGGT*GCA*GATGATGACATTTAT-3′
- E317D: 5′ pGGCTGGGGAGGT*GAC*GATGATGACATTTAT-3′
- D318N: 5′ pGGGGCTGGGGAGGTGAA*AAT*GATGACATTTA-TAAC-3′
- D318A: 5′ pGGCTGGGGAGGTGAA*GCT*GATGACATTTAT-3′
- D318E: 5′ pGGCTGGGGAGGTGAA*GAA*GATGACATTTAT-3′
- D319N: 5′ pGGGGAGGTGAAGAT*AAT*GACATTTATAACAG-ATTAGC-3′
- D319A: 5′ pGGCTGGGGAGGTGAAGAT*GCT*GACATTTAT-3′
- D319E: 5′ pGGCTGGGGAGGTGAAGAT*GAA*GACATTTAT-3′
- D320N: 5′ pGGGGAGGTGAAGATGAT*AAC*ATTTATAACAG-ATTAGC-3′
- D320E: 5′ pGGGGAGGTGAAGATGAT*GAA*ATTTATAACAG-ATTAGC-3′
- M344A: 5′ pGTGATCGGGAAGACGCGC*GCG*ATCCGCCACT-CGAGAGAGAAGAAA-3′
- M344Q: 5′ pGTGATCGGGAAGACGCGC*CAG*ATCCGCCACT-CGAGAGACAAGAAA-3′
- H347E: 5′ pGTGATCGGGAAGACGCGCATGATCCGC*GAA*T-CGAGAGACAAGAAA-3′
- H347D: 5′ pGTGATCGGGAAGACGCGCATGATCCGC*GAC*T-CGAGAGACAAGAAA-3′
- H347N: 5′ pGTGATCGGGAAGACGCGCATGATCCGC*AAC*T-CGAGAGACAAGAAA-3′
- H347Q: 5′ pGTGATCGGGAAGACGCGCATGATCCGC*CAG*T-CGAGAGACAAGAAA-3′

The mutated residues are shown in italics. The potential mutants were selected after observing changes in the restriction enzyme patterns. Mutations were confirmed by DNA sequencing using Sequenase version 2.0 (USB, Cleveland, OH).

Preparation and purification of wild-type and mutant proteins

The *E. coli* XL2-Blue ultracompetent and BL21 (DE3) / pLysS competent cells were transformed with the pET vector derivatives per manufacturer's protocols. The transformed cells were grown overnight with shaking at 37°C in an LB broth containing 50 μg ml^{-1} ampicillin. The overnight cultures were induced with 0.4 mM ispropylthiogalactoside (IPTG) for 4 h. After IPTG induction, the inclusion bodies were isolated from the bacterial pellet essentially as described (Boeggeman *et al.*, 1993). After washing four times with a suspension buffer containing 25% (w/v) sucrose, the inclusion bodies were washed with 1× phosphate buffered saline buffer. From a liter of induced bacterial culture, one generally gets ~80–100 mg of purified inclusion bodies. Our laboratory has developed a protocol to generate active recombinant β4Gal-T1 from these inclusion bodies using oxido-shuffling agents during renaturation (Boeggeman *et al.*, 1993). On dilution with guanidine-HCl and subsequent dialysis, a portion of the folded protein was found to precipitate in the form of aggregates. To increase the protein yields, we modified this protocol as follows: 100 mg of inclusion bodies were dissolved in 10 ml of 5 M guanidine-HCl containing 0.3 M sodium sulfite. One milliliter of a 50 mM disodium 2-nitro-5-thiosulfobenzoate solution is added to sulfonate the free thiols in the proteins. Completion of sulfonation was judged by a color change from deep orange to pale yellow. The sulfonated protein was diluted 10-fold in water, precipitated, collected by centrifugation at 10,000 × *g*, and washed four times with water to remove any remaining sulfonating agent. The protein was redissolved in 5 M guanidine-HCl, to a protein concentration of 1 mg/ml, with OD_{275} of 1.9–2.0. The protein solution was diluted 10-fold in a solution containing 100 μg/ml β4Gal-T1, 50 mM Tris–HCl (pH 8.0), 5 mM ethylenediamine tetra-acetic acid, 0.5M guanidine-HCl, 4 mM cysteamine, and 2 mM cystamine. The protein was renatured for 48 h at 4°C, dialyzed, and concentrated using ultrafiltration membranes (Amicon, Beverly, MA). The advantage of this method is that the precipitated protein can be resulfonated to generate more of active β4Gal-T1. Using this procedure, the yield was 3–5 mg of pure and active β4Gal-T1 from 100 mg sulfonated protein per liter of folding solution. The precast Novex gels were used for SDS–PAGE analysis, and the protein bands visualized with Coomassie blue. Protein concentrations were measured with the Bio-Rad protein dye reagent with bovine serum albumin as the standard.

β4Gal-T1 enzyme assays and kinetic analysis

The *in vitro* assay for β4Gal-T1 enzyme activity was performed as described (Boeggeman *et al.*, 1995). The activities were measured using ^{3}H-labeled-UDP-Gal and the sugar acceptor GlcNAc. Typically, a 100-µl incubation mixture contained 25 mM GlcNAc, 5 mM $MnCl_2$, 0.05 mM UDP-Gal, 5 mM Tris–HCl (pH 8.0), 0.5% Triton X-100, 10–20 ng of β4Gal-T1, and 0.5 µCi ^{3}H-UDP-Gal. A reaction without GlcNAc was used as a control. The incubation was carried out at 30°C for 15 min and terminated by the addition of 200 µl cold water. The incubation mixture was added to a column containing 0.5 ml bed volume AG1-X8 cation resin and was washed with cold water. The flow-through was diluted in 20 ml Biosafe scintillation fluid and the radioactivity measured in a Beckman counter. The mutated proteins showed reduced but detectable enzymatic activities as compared to the wild-type recombinant β4Gal-T1.

The kinetic parameters for UDP-Gal and GlcNAc were determined using double substrate kinetics at a fixed Mn^{2+} concentration of 10 mM, with concentrations of UDP-Gal varying between 0.005 and 2 mM and at fixed GlcNAc concentration of 1–50 mM. Data were analyzed for a two-substrate system by fitting to an equation for sequential symmetrical initial velocity pattern, Equation 1 (Zhang *et al.*, 1999), (ordered or random equilibrium mechanism); or to an equation for asymmetric initial velocity pattern, Equation 2 (Zhang *et al.*, 1999), for a double-displacement or ping-pong mechanism.

$$(1) \quad <= (V_{max} * [A] * [D]) / (K_{id} * K_{md}) + (K_{md} * [A]) + (K_{ma} * [D]) + ([A] * [D])$$

$$(2) \quad <= (V_{max} * [A] * [D]) / (K_{ma} * [D]) + (K_{md} * [A]) + ([A] * [D])$$

In the equations, [*D*] represents the concentration of the donor; [*A*] the concentration of the acceptor; K_{ma} and K_{md}, the true K_m for the acceptor and the donor, respectively; and K_{id} the dissociation constant for the donor. The Enzfitter (Biosoft), a nonlinear curve-fitting program for Windows was used to obtain the kinetic parameters from the fitted curves using Equations 1 and 2.

For determining metal binding constants the rate of *N*-acetyllactosamine synthesis was measured at various concentrations of metal ions at fixed GlcNAc (20 mM) and UDP-Gal concentrations (0.2 mM). Mn^{2+} and Co^{2+} concentrations were varied between 0 and 5 mM. The data were fitted to Equation 3 (Zhang *et al.*, 1999), describing two-metal binding sites, or to Equation 4 (Zhang *et al.*, 1999), describing a single-metal binding site.

$$(3) \quad <= [M] * [(V_1 * K_2) + (V_2 * [M])] / [(K_1 * K_2) + (K_2 * [M] + [M]^2)]$$

$$(4) \quad <= (V * [M]) / (K_d + [M])$$

The metal binding to site 1 with high affinity (K_1) is associated with low velocity (V_1) and the binding to the low-affinity site 2 with an apparent K_d of K_2 is associated with high velocity (V_2). [*M*] is the concentration of either Mn^{2+} or Co^{2+}.

Binding of recombinant proteins to UDP-affinity column

The binding to the UDP-agarose column was carried out at 4°C. Columns containing 1 ml bed volume of UDP-agarose were preequilibrated with a 25 mM cacodylic buffer, pH 7.6, containing variable amounts of $MnCl_2$ (25, 5, or 1 mM). The renatured protein solutions (0.5 mg) were adjusted to the preequilibration buffer conditions and applied to the columns. After loading of the samples, the pass-through was recycled again. The pass-through was analyzed for the unbound protein (U). The columns were washed 3× with 1-ml portions of equilibration buffer (W). The elution buffer consisted of 25 mM cacodylic buffer, pH 7.6, containing 25 mM ethylenediamine tetra-acetic acid and 1 M NaCl. For elution of the proteins, 0.5-ml fractions (E) were collected from the columns, and aliquots were analyzed by SDS–PAGE.

Acknowledgments

We thank B. Ramakrishnan for many helpful suggestions and discussions during the course of this work and S. Kumar and P. V. Balaji for critical readings of the manuscript. The content of this publication does not necessarily reflect the view or policies of the Department of Health and Human Services, nor does mention of trade names, commercial products, or organization imply endorsement by the U.S. government. This project was funded in part with federal funds from the NCI, NIH, under contract no. NO1-CO-12400.

Abbreviations

Gal-T, galactosyltransferase; GlcNAc, *N*-acetylglucosamine; IPTG, ispropylthiogalactoside; LA, lactalbumin; LB, Luria-Bertani; SDS–PAGE, sodium dodecyl sulfate–polyacrylamide gel electrophoresis.

References

Almeida, R., Amado, M., David, L., Levery, S.B., Holmes, E.H., Merkx, G., van Kessel, A.G., Rygaard, E., Hassan, H., Bennett, E., and Clausen, H. (1997) A family of human beta4-galactosyltransferases. Cloning and expression of two novel UDP-galactose:beta-N-acetylglucosamine beta1, 4-galactosyltransferases, beta4Gal-T2 and beta4Gal-T3. *J. Biol. Chem.*, **272**, 31979.

Almeida, R., Levery, S.B., Mandel, U., Kressel, H., Schwientek, T., Bennett, E.P., and Clausen, H. (1999) Cloning and expression of a proteoglycan UDP-galactose:beta-xylose beta1, 4-galactosyltransferase I. A seventh member of the human beta4-galactosyltransferase gene family. *J. Biol. Chem.*, **274**, 26165.

Amado, M., Almeida, R., Schwientek, T., and Clausen, H. (1999) Identification and characterization of large galactosyltransferase gene families: galactosyltransferases for all functions. *Biochim. Biophys. Acta*, **1473**, 35.

Aoki, D., Appert, H.E., Johnson, D., Wong, S.S., and Fukuda, M.N. (1990) Analysis of the substrate binding sites of human galactosyltransferase by protein engineering. *EMBO J.*, **9**, 3171.

Ausubel, F.M., Brent, R., Kinstom, R.E., Moore, D.D., Smith, J.A., Seidman, J.G., and Struhl, K. (1987) *Current protocols in molecular biology*. Wiley, New York.

Baumann, U., Bauer, M., Letoffe, S., Delepelaire, P., and Wandersman, C. (1995) Crystal structure of a complex between *Serratia marcescens* metallo-protease and an inhibitor from *Erwinia chrysanthemi*. *J. Mol. Biol.*, **248**, 653.

Bell, J.E., Beyer, T.A., and Hill, R.L. (1976) The kinetic mechanism of bovine milk galactosyltransferase. The role of alpha-lactalbumin. *J. Biol. Chem.*, **251**, 3003.

Boeggeman, E. and Qasba, P.K. (1998) Identification of three sequence regions, two of which contain DXD motifs involved in the catalytic activity of β-1, 4 galactosyltransferase. *FASEB J.*, **12**, 8.

Boeggeman, E.E., Balaji, P.V., and Qasba, P.K. (1995) Functional domains of bovine beta-1, 4 galactosyltransferase. *Glycoconj. J.*, **12**, 865.

Boeggeman, E.E., Balaji, P.V., Sethi, N., Masibay, A.S., and Qasba, P.K. (1993) Expression of deletion constructs of bovine beta-1, 4-galactosyltransferase in *Escherichia coli*: importance of Cys134 for its activity. *Prot. Eng.*, **6**, 779.

Breton, C., Bettler, E., Joziasse, D.H., Geremia, R.A., and Imberty, A. (1998) Sequence-function relationships of prokaryotic and eukaryotic galactosyltransferases. *J. Biochem. (Tokyo)*, **123**, 1000.

Busch, C., Hofmann, F., Selzer, J., Munro, S., Jeckel, D., and Aktories K. (1998) A common motif of eukaryotic glycosyltransferases is essential for the enzyme activity of large clostridial cytotoxins. *J. Biol. Chem.*, **273**, 19566.

Clymer, D.J., Geren, C.R., and Ebner, K.E. (1976) Ultraviolet photoinactivation of galactosyltransferase. Protection by substrates. *Biochemistry*, **15**, 1093.

D'Agostaro, G., Bendiak, B., and Tropak, M. (1989) Cloning of cDNA encoding the membrane-bound form of bovine beta 1, 4-galactosyltransferase. *Eur. J. Biochem.*, **183**, 211.

Gastinel, L.N., Cambillau, C., and Bourne, Y. (1999) Crystal structures of the bovine beta4galactosyltransferase catalytic domain and its complex with uridine diphosphogalactose. *EMBO J.*, **18**, 3546.

Geren, C.R., Magee, S.C., and Ebner, K.E. (1975) Circular dichroism changes in galactosyltransferase upon substrate binding. *Biochemistry*, **14**, 1461.

Hatanaka, Y., Ishiguro, M., Hashimoto, M., Gastinel, L.N., and Nakagomi, K. (2001) A model of photoprobe docking with beta1, 4-galactosyltransferase identifies a possible carboxylate involved in glycosylation steps. *Bioorg. Med. Chem. Lett.*, **11**, 411.

Hill, R.L. (1979) Glycosyltransferases in analysis of oligosaccharide structure and function. *UCLA Forum Med. Sci.*, **21**, 63.

Hodson, N., Griffiths, G., Cook, N., Pourhossein, M., Gottfridson, E., Lind, T., Lidholt, K., and Roberts, I.S. (2000) Identification that KfiA, a protein essential for the biosynthesis of the *Escherichia coli* K5 capsular polysaccharide, is an alpha -UDP-GlcNAc glycosyltransferase. The formation of a membrane-associated K5 biosynthetic complex requires KfiA, KfiB, and KfiC. *J. Biol. Chem.*, **275**, 27311.

Keiderling, T.A., Silva, R.A.G.D., Yoder, G., and Dukor, R.K. (1999) Vibrational circular dichroism spectroscopy of selected oligopeptide conformations. *Bioorg. Med. Chem.*, **7**, 133.

Khatra, B.S., Herries, D.G., and Brew, K. (1974) Some kinetic properties of human-milk galactosyl transferase. *Eur. J. Biochem.*, **44**, 537.

Lo, N.W., Shaper, J.H., Pevsner, J., and Shaper, N. (1998) The expanding beta 4-galactosyltransferase gene family: messages from the databanks. *Glycobiology*, **8**, 517.

Masibay, A.S. and Qasba, P.K. (1989) Expression of bovine beta-1, 4-galactosyltransferase cDNA in COS-7 cells. *Proc. Natl Acad. Sci. USA*, **86**, 5733.

Messerschmidt, A., Prade, L., Kroes, S.J., Sanders-Loehr, J., Huber, R., and Canters, G.W. (1998) Rack-induced metal binding vs. flexibility: Met121His azurin crystal structures at different pH. *Proc. Natl Acad. Sci. USA*, **95**, 3443.

Morrison, J.F. and Ebner, K. E. (1971a) Studies on galactosyltransferase. Kinetic effects of lactalbumin with N-acetylglucosamine and glucose as galactosyl group acceptors. *J. Biol. Chem.*, **246**, 3992.

Morrison, J.F. and Ebner, K.E. (1971b) Studies on galactosyltransferase. Kinetic investigations with N-acetylglucosamine as the galactosyl group acceptor. *J. Biol. Chem.*, **246**, 3977.

Narimatsu, H., Sinha, S., Brew, K., Okayama, H., and Qasba, P.K. (1986) Cloning and sequencing of cDNA of bovine N-acetylglucosamine (beta 1-4) galactosyltransferase. *Proc. Natl Acad. Sci. USA*, **83**, 4720.

Nomura, T., Takizawa, M., Aoki, J., Arai, H., Inoue, K., Wakisaka, E., Yoshizuka, N., Imokawa, G., Dohmae, N., Takio, K., and others. (1998) Purification, cDNA cloning, and expression of UDP-Gal: glucosylceramide beta-1, 4-galactosyltransferase from rat brain. *J. Biol. Chem.*, **273**, 13570.

O'Keeffe, E.T., Hill, R.L., and Bell, J.E. (1980) Active site of bovine galactosyltransferase: kinetic and fluorescence studies. *Biochemistry*, **19**, 4954.

Okajima, T., Yoshida, K., Kondo, T., and Furukawa, K. (1999) Human homolog of *Caenorhabditis elegans* sqv-3 gene is galactosyltransferase I involved in the biosynthesis of the glycosaminoglycan-protein linkage region of proteoglycans. *J. Biol. Chem.*, **274**, 22915.

Paulson, J.C. and Colley, K.J. (1989) Glycosyltransferases. *Structure*, localization, and control of cell type-specific glycosylation. *J. Biol. Chem.*, **264**, 17615.

Powell, J.T. and Brew, K. (1974) The preparation and characterization of two forms of bovine galactosyl transferase. *Eur. J. Biochem.*, **48**, 217.

Powell, J.T. and Brew, K. (1976) Metal ion activation of galactosyltransferase. *J. Biol. Chem.*, **251**, 3645.

Ramakrishnan, B. and Qasba, P.K. (2001) Crystal structure of lactose synthase reveals a large conformational change in its catalytic component, the beta1, 4-galactosyltransferase-I. *J. Mol. Biol.*, **310**, 205.

Ramakrishnan, B., Balaji, P.V., and Qasba, P.K. (2002) Crystal structure of β1, 4-galactosyl-transferase complex with UDP-Gal reveals an oligosaccharide acceptor-binding site. *J. Mol. Biol.*, in press.

Ramakrishnan, B., Shah, P.S., and Qasba, P.K. (2001) Alpha-lactalbumin (LA) stimulates milk beta-1, 4-galactosyltransferase I (beta 4Gal-T1) to transfer glucose from UDP-glucose to N-acetylglucosamine. Crystal structure of beta 4Gal-T1 x LA complex with UDP-Glc. *J. Biol. Chem.*, **276**, 37665.

Russo, R.N., Shaper, N.L., and Shaper, J.H. (1990) Bovine beta 1-4-galactosyltransferase: two sets of mRNA transcripts encode two forms of the protein with different amino-terminal domains. *In vitro* translation experiments demonstrate that both the short and the long forms of the enzyme are type II membrane-bound glycoproteins. *J. Biol. Chem.*, **265**, 3324.

Sato, T., Furukawa, K., Bakker, H., Van den Eijnden, D.H., and Van Die, I. (1998a) Molecular cloning of a human cDNA encoding beta-1, 4-galactosyltransferase with 37% identity to mammalian UDP-Gal:GlcNAc beta-1, 4-galactosyltransferase. *Proc. Natl Acad. Sci. USA*, **95**, 472.

Sato, T., Aoki, N., Matsuda, T., and Furukawa, K. (1998b) Differential effect of alpha-lactalbumin on beta-1, 4-galactosyltransferase IV activities. *Biochem. Biophys. Res. Commun.*, **244**, 637.

Schwientek, T., Almeida, R., Levery, S.B., Holmes, E.H., Bennett, E., and Clausen, H. (1998) Cloning of a novel member of the UDP-galactose:beta-N-acetylglucosamine beta1, 4-galactosyltransferase family, beta4Gal-T4, involved in glycosphingolipid biosynthesis. *J. Biol. Chem.*, **273**, 29331.

Shaper, N.L., Shaper, J.H., Meuth, J.L., Fox, J.L., Chang, H., Kirsch, I.R., and Hollis, G.F. (1986) Bovine galactosyltransferase: identification of a clone by direct immunological screening of a cDNA expression library. *Proc. Natl Acad. Sci. USA*, **83**, 1573.

Shibayama, K., Ohsuka, S., Sato, K., Yokoyama, K., Horii, T., and Ohta, M. (1999) Four critical aspartic acid residues potentially involved in the catalytic mechanism of *Escherichia coli* K-12 WaaR. *FEMS Microbiol. Lett.*, **174**, 105.

Shibayama, K., Ohsuka, S., Tanaka, T., Arakawa, Y., and Ohta M. (1998) Conserved structural regions involved in the catalytic mechanism of *Escherichia coli* K-12 WaaO (RfaI). *J. Bacteriol.*, **180**, 5313.

Sinnott, M.L. (1990) Glycosyl group transfer. *Chem. Rev.*, **90**, 1171.

Unligil, U.M., Zhou, S., Yuwaraj, S. M., Schachter, H., and Rini, J.M. (2000) X-ray crystal structure of rabbit N-acetylglucosaminyltransferase I: catalytic mechanism and a new protein superfamily. *EMBO J.*, **19**, 5269.

Wiggins, C.A.R. and Munro, S. (1998) Activity of the yeast MNN1 alpha-1, 3-mannosyltransferase requires a motif conserved in many other families of glycosyltransferases. *Proc. Natl Acad. Sci. USA*, **95**, 7945.

Yuan, Y.P., Schultz, J., Mlodzik, M., and Bork, P. (1997) Secreted fringe-like signaling molecules may be glycosyltransferases. *Cell*, **88**, 9.

Zhang, Y., Malinovskii, V.A., Fiedler, T.J., and Brew, K. (1999) Role of a conserved acidic cluster in bovine beta1, 4 galactosyltransferase-1 probed by mutagenesis of a bacterially expressed recombinant enzyme. *Glycobiology*, **9**, 815.